

Cite this: *RSC Sustainability*, 2023, 1, 640

# Engineering a bromophenol derivative for rapid detection of $\text{Hg}^{2+}/\text{CH}_3\text{Hg}^+$ in both environmental and biological samples through a unique activation process†

Tapendu Samanta, Narayan Das, Diptendu Patra, Pawan Kumar  and Raja Shunmugam \*

Reaction-based sensory systems are always preferred for detecting  $\text{Hg}^{2+}$  and its organic form,  $\text{CH}_3\text{Hg}^+$ . A simple bromophenol derivative (BDT) has been developed as a cheap, small and ultrasensitive sensor for both  $\text{Hg}^{2+}$  and  $\text{CH}_3\text{Hg}^+$  ions with rapid detection ability. The transformation of the 1,3-dithiolane segment to the formyl group has been utilized here as a key feature for the turn "off-on" fluorescence response due to the activation of the ESIPT process during the detection of the analytes. Most of the 1,3-dithiolane systems required a long response time for  $\text{CH}_3\text{Hg}^+$ , but BDT has been demonstrated as an excellent system that required a low response time to detect the organic form of mercury. Having a limit of detection (LOD) value of 3.8 nM and 0.8  $\mu\text{M}$  towards  $\text{Hg}^{2+}$  and  $\text{CH}_3\text{Hg}^+$  respectively in an aqueous medium, BDT served as an excellent detection probe with environmental detection capability. It has been supported by ICP-MS analysis of commercially available vermilion. BDT has been utilized to detect  $\text{Hg}^{2+}$  in a biological system with excellent efficiency along with ecological and real sample analysis. Furthermore, the desulfurization process triggered by  $\text{Hg}^{2+}$  has been proved using  $^1\text{H}$  NMR analysis and spectroscopic fluorescence techniques. These observations encouraged us to claim BDT as an excellent cheap and easily synthesizable efficient tool for detecting inorganic and organic mercury in controlled, environmental, and biological systems.

Received 9th January 2023  
Accepted 17th March 2023

DOI: 10.1039/d3su00012e

rsc.li/rscsus

## Sustainability spotlight

The bioaccumulation of  $\text{Hg}(\text{II})$  and methylmercury ( $\text{CH}_3\text{Hg}^+$ ), due to their solid binding tendency to thiols of different enzymes and proteins, caused several physiological issues such as kidney damage, central nervous system damage, motion disorder, and even death. Therefore, to avoid the hazardous effect of  $\text{Hg}^{2+}$  and  $\text{CH}_3\text{Hg}^+$ , an upper limit of  $\text{Hg}^{2+}$  has been set as 10 nM by the U.S. Environmental Protection Agency (EPA). By this virtue, the development of selective and sensitive detection strategies for mercury in environmental and living systems is an important issue to be addressed by researchers. However, traditional methods need expensive instrumentation and complicated experimental procedures despite high sensitivity and precision. In this respect, reaction-based probes are preferable due to their high selectivity and sensitivity. To the best of our knowledge, herein, we report the smallest 1,3-dithiolane-based probe BDT, where a diformyl system (BDA) has been modified using a 1,2-ethanethiol segment. BDT showed excellent selectivity and sensitivity towards  $\text{Hg}^{2+}$  and methylmercury ions in an aqueous environment and biological system comprehensively.

## Introduction

The toxic effect of mercury is well known for Minamata disease and poisoning in Iraq.<sup>1–3</sup> Mercury contamination is mainly originated from the release of mercury from different chemical

industries.<sup>4,5</sup> Uncontrolled release has increased the amount of mercury in surface water and heavily affects humankind throughout the world.<sup>6</sup> The bioaccumulation of  $\text{Hg}(\text{II})$  and methylmercury ( $\text{CH}_3\text{Hg}^+$ ) due to their solid binding tendency to thiols of different enzymes and proteins caused several physiological issues such as kidney damage, central nervous system damage, motion disorder, and even death.<sup>7,8</sup> On the other hand, organic species of mercury are known to be highly toxic.<sup>9,10</sup> Among different organic mercury species,  $\text{CH}_3\text{Hg}^+$  is a commonly known toxicant that is significantly more harmful than the inorganic  $\text{Hg}^{2+}$  ions. It is frequently found in marine seafood. Compared to  $\text{Hg}^{2+}$ ,  $\text{CH}_3\text{Hg}^+$  can easily penetrate biological membranes and the blood-brain barrier and thus affect

Polymer Research Centre, Department of Chemical Sciences, Indian Institute of Science Education and Research, Kolkata, West Bengal, 741246, India. E-mail: email-sraja@iiserkol.ac.in

† Electronic supplementary information (ESI) available: Materials and methods, synthetic procedures, NMR and ESI-MS spectra, UV-vis and fluorescence spectra, linear plots, time dependent studies, table for comparison among reported literature studies, and real sample analysis summary table. See DOI: <https://doi.org/10.1039/d3su00012e>



the nervous system.<sup>11</sup> To avoid the hazardous effect of  $\text{Hg}^{2+}$  and  $\text{CH}_3\text{Hg}^+$ , an upper limit of  $\text{Hg}^{2+}$  has been set as 10 nM by the U.S. Environmental Protection Agency (EPA).<sup>12</sup> By this virtue, the development of selective and sensitive detection strategies for mercury in environmental and living systems is an important issue to be addressed by researchers. Several traditional methods such as atomic absorption spectroscopy (AAS), inductively coupled plasma mass spectrometry (ICP-MS), atomic fluorescence spectrometry (AFS), chromatographic techniques, and voltammetry studies are available for the detection of mercury with high sensitivity and accuracy.<sup>10–20</sup> Despite high sensitivity and precision, traditional methods need expensive instrumentation and complicated experimental procedures.<sup>21–24</sup> However, the spectroscopic fluorescence technique has emerged as a point of interest in recent times due to its comprehensive sensitivity, response, and easy sample preparation process.<sup>25–29</sup> In the last few years, most fluorescent probes for  $\text{Hg}^{2+}$  were designed using heteroatom-containing ligand systems. However, these kinds of probes suffer from low selectivity due to reversible complexation and interference from different ions.<sup>30–32</sup> In this respect, reaction-based probes are preferable due to their high selectivity and sensitivity, as an Hg-triggered reaction with a probe leads to a new fluorogenic or chromogenic substance formation with unique spectral properties.<sup>33</sup> The deprotection of thioacetals to aldehydes or ketones, promoted by  $\text{Hg}^{2+}$  is one of the most utilized reactions to design a chemodosimeter with high selectivity.<sup>34–36</sup> The formation of thioacetals can be achieved simply by reacting thiols with aldehyde or ketone segments of any molecule and can be deprotected explicitly by  $\text{Hg}^{2+}$  ions.<sup>37</sup> Besides, very few reaction-based probes have been reported for methylmercury, to date and most of the probes require a high concentration of  $\text{CH}_3\text{Hg}^+$  and a considerable reaction time due to the minor thiophilic nature of methylmercury.<sup>38–41</sup>

Generally, three well-known fluorescence mechanisms, such as PET (Photoinduced Electron Transfer), FRET (Förster Resonance Energy Transfer), and ICT (Internal Charge Transfer), are explored vastly for the development of sensor molecules. However, excited-state intramolecular proton transfer (ESIPT) based probes have received great attention in terms of applications due to their unique photophysical properties such as large Stokes shift, good photostability, and high quantum yield.<sup>42,43</sup>

By this virtue, to the best of our knowledge, herein, we report the smallest 1,3-dithiolane based probe **BDT**, where a diformyl system (**BDA**) has been modified using a 1,2-ethanedithiol segment. **BDT** has been designed so that the  $\text{Hg}^{2+}$  triggered deprotection of the 1,3-dithiolane moiety to an aldehyde can turn on the ESIPT process to produce a unique emission signal.

2-(2'-Hydroxyphenyl) benzothiazole (HBT) is a well-known ESIPT active fluorophore used as the basic unit for developing different sensors throughout the years, and  $-\text{OH}$  and benzothiazole moieties are involved in the proton transfer process.<sup>44,45</sup> But in the case of **BDT**,  $\text{Hg}^{2+}$  and  $\text{CH}_3\text{Hg}^+$  promoted thioacetal deprotection and produced a basic keto-enol tautomerizing unit that activated the ESIPT process by showing intense intensity green fluorescence as output. Moreover, a single benzene ring containing **BDT** showed excellent selectivity and sensitivity towards  $\text{Hg}^{2+}$  and methylmercury ions in an aqueous environment and biological system comprehensively.

## Experimental section

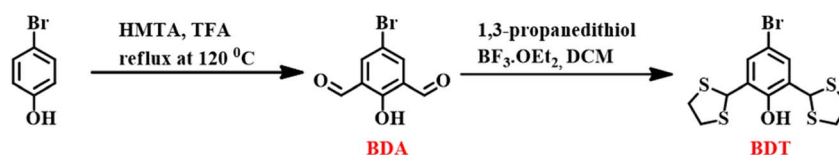
We have synthesized **BDT** in two steps starting from 4-bromophenol (Scheme 1, ESI†). Initially, 4-bromophenol has been converted to a dialdehyde system (**BDA**) using the Duff reaction where hexamethylenetetramine (HMTA) and TFA have been used as reagents. In the second step, **BDA** has been converted to **BDT** using 1,3-ethanedithiol. All these products have been successfully characterized using  $^1\text{H}$  NMR,  $^{13}\text{C}$  NMR, and ESI-MS techniques. The detailed synthetic methods and characterization of each compound have been discussed in the ESI (Fig. S1–S6†).

## Results and discussion

### Photophysical properties of **BDT**

The initial photophysical study of **BDT** showed absorbance maxima at 306 nm in a DMSO/PBS (4 : 1, v/v, pH 7.4) medium. However, the addition of  $\text{Hg}^{2+}$  resulted in the appearance of a new absorbance maximum at 350 nm (Fig. S7, ESI†). In terms of fluorescence emission, **BDT** showed an emission maximum of around 526 nm upon adding an  $\text{Hg}^{2+}$  ion, which was absent initially (Fig. S8, ESI†). The selectivity of **BDT** was thoroughly investigated using fluorescence spectroscopy for various metal ions such as  $\text{Na}^+$ ,  $\text{K}^+$ ,  $\text{Li}^+$ ,  $\text{Mg}^{2+}$ ,  $\text{Ca}^{2+}$ ,  $\text{Cu}^{2+}$ ,  $\text{Zn}^{2+}$ ,  $\text{Pb}^{2+}$ ,  $\text{Co}^{2+}$ ,  $\text{Fe}^{2+}$ ,  $\text{Cd}^{2+}$ ,  $\text{Sn}^{2+}$ ,  $\text{Fe}^{3+}$ ,  $\text{Cr}^{3+}$  and  $\text{Hg}^{2+}$  in a DMSO/PBS (4 : 1, v/v, pH 7.4) medium, where the 526 nm emission band was observed only for the  $\text{Hg}^{2+}$  ion (Fig. 1A). Selectivity studies of **BDT** (Fig. 1B) established the precise nature of our probe towards  $\text{Hg}^{2+}$  ions, which is the beneficial aspect of reaction-based systems. Due to the activation of the ESIPT phenomenon, **BDT** showed green emissive nature in the presence of  $\text{Hg}^{2+}$  but remained non-emissive for other analytes, as depicted in Fig. 1C.

After a successful investigation of the selectivity of **BDT**, we have determined the response dynamics towards  $\text{Hg}^{2+}$  under the same experimental conditions used in the initial photophysical experiments. A rapid response time of 1 minute,



Scheme 1 Synthesis procedure of **BDT**.



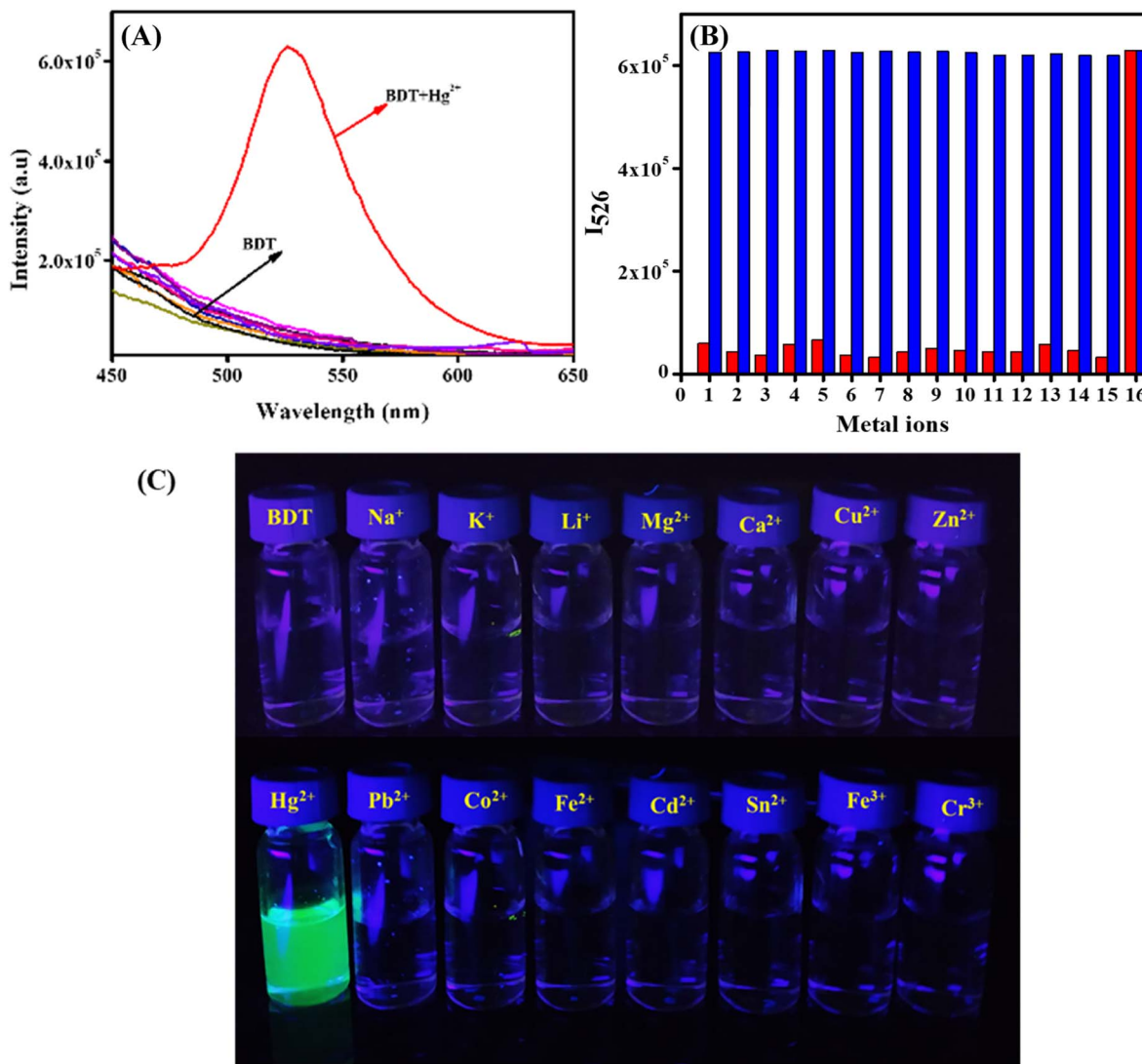


**Fig. 1** (A) Fluorescence spectra of BDT (10 μM) and (B) corresponding comparative bar plot of  $I_{526 \text{ nm}}$  in the presence of different metal ions in a DMSO/PBS buffer (4 : 1, v/v, pH 7.4) medium: (1) blank, (2) Na<sup>+</sup>, (3) K<sup>+</sup>, (4) Li<sup>+</sup>, (5) Mg<sup>2+</sup>, (6) Ca<sup>2+</sup>, (7) Cu<sup>2+</sup>, (8) Zn<sup>2+</sup>, (9) Pb<sup>2+</sup>, (10) Co<sup>2+</sup>, (11) Fe<sup>2+</sup>, (12) Cd<sup>2+</sup>, (13) Sn<sup>2+</sup>, (14) Fe<sup>3+</sup>, (15) Cr<sup>3+</sup>, and (16) Hg<sup>2+</sup>; red columns = BDT + metal ions; blue columns = BDT + metal ions + Hg<sup>2+</sup>. (C) Pictorial representation of BDT solutions in the presence of different analytes under a hand-held UV lamp ( $\lambda_{\text{ex}} = 350 \text{ nm}$ ).

required for a complete reaction between BDT and Hg<sup>2+</sup>, was evident from the time-dependent fluorescence studies (Fig. S9, ESI†). This detection kinetics confirmed the 1 minute incubation time of Hg<sup>2+</sup> with BDT for all future spectroscopic experiments. Reaction dynamics and selectivity studies confirmed the novelty of BDT towards detecting Hg<sup>2+</sup> ions in terms of rapid response and high specificity. The quantum yield of BDT in the presence of Hg<sup>2+</sup> has been evaluated using quinine sulfate as reference (eqn (1), ESI†). The value of quantum yield for BDT is calculated to be 0.11.

Sensitivity and detection parameters are essential for a probe to be an excellent candidate for sensing any analyte. Towards this, we have carried out a fluorescence titration study of BDT with varying concentrations of Hg<sup>2+</sup> in a 4 : 1 DMSO/PBS (v/v, pH = 7.4) medium. As expected, the emission intensity of BDT at 526 nm increased gradually with the progressive addition of

Hg<sup>2+</sup> ions (0–60 μM) (Fig. 2A), with a change in emission from colourless to green (Fig. 2A, inset). A drastic 33-fold increase in emission intensity at 526 nm till two equivalent Hg<sup>2+</sup> addition followed by plateau formation (Fig. S10, ESI†) convincingly suggested the gradual desulfurization process. The absorption studies of BDT with changing concentrations of Hg<sup>2+</sup> (0–100 μM) (Fig. S11, ESI†) also exhibited a similar kind of spectroscopic change which again supported our claim of the desulfurization process.

From the titration study, a calibration plot has been constructed in 0–20 μM for BDT. The linear plot of intensity at 526 nm with the concentration of Hg<sup>2+</sup> showed excellent linearity with an adjacent  $R^2$  value of 0.99025. This linear plot has been utilized to calculate the theoretical lowest detection limit (LOD =  $3\sigma/K$ ) of BDT with a values of 3.8 nM for Hg<sup>2+</sup>, which is well comparable with other desulfurization based reported



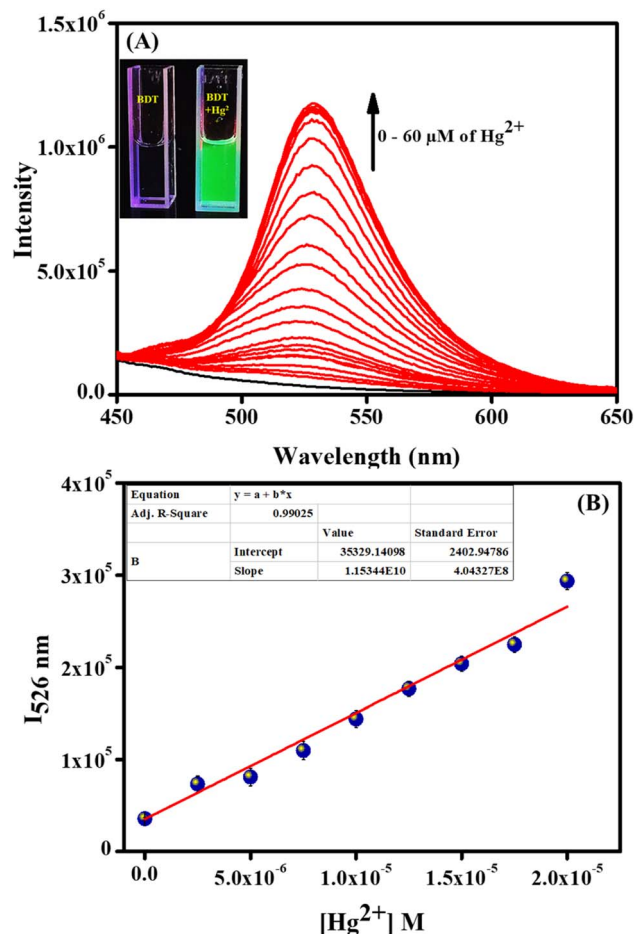


Fig. 2 Fluorescence spectra of BDT (20  $\mu\text{M}$ ), obtained (A) upon addition of  $\text{Hg}^{2+}$  (0–60  $\mu\text{M}$ ) in DMSO/PBS buffer (4 : 1, v/v, pH 7.4) solution (inset: picture of BDT solution before and after addition of  $\text{Hg}^{2+}$  ions under a hand-held UV lamp of 365 nm) and corresponding calibration plot of (B)  $I_{526 \text{ nm}}$  vs concentration of  $\text{Hg}^{2+}$  ions (0–20  $\mu\text{M}$ ).

probes (Table S1, ESI<sup>†</sup>) and well below the permissible limit of 10 nM.

### Detection of $\text{CH}_3\text{Hg}^+$ by BDT

Reaction-based probes of  $\text{Hg}^{2+}$  are also reactive towards  $\text{CH}_3\text{Hg}^+$  in a similar mechanism. In this context, we carried out the sensing behavior studies of BDT towards the  $\text{CH}_3\text{Hg}^+$  ion under identical experimental conditions. The initial time-dependent studies confirmed the rapid detection ability of BDT towards  $\text{CH}_3\text{Hg}^+$  in DMSO/PBS (4 : 1, v/v, pH = 7.4) (Fig. S12, ESI<sup>†</sup>). Furthermore, a quick response time of BDT defined the excellent factor for detecting  $\text{CH}_3\text{Hg}^+$  compared to other various reported probes (Table S1, ESI<sup>†</sup>). Furthermore, a gradual increase in the  $I_{505 \text{ nm}}$  value was observed for BDT upon progressive addition of  $\text{CH}_3\text{Hg}^+$  ions (Fig. 3A). Titrimetric results have been utilized to construct the calibration curve (Fig. 3B) in the concentration of 0–90  $\mu\text{M}$  for methylmercury. This linear plot with an  $R^2$  value of 0.98932 has been utilized to calculate the LOD value of 0.8  $\mu\text{M}$  for BDT towards  $\text{CH}_3\text{Hg}^+$  in a controlled experimental medium.

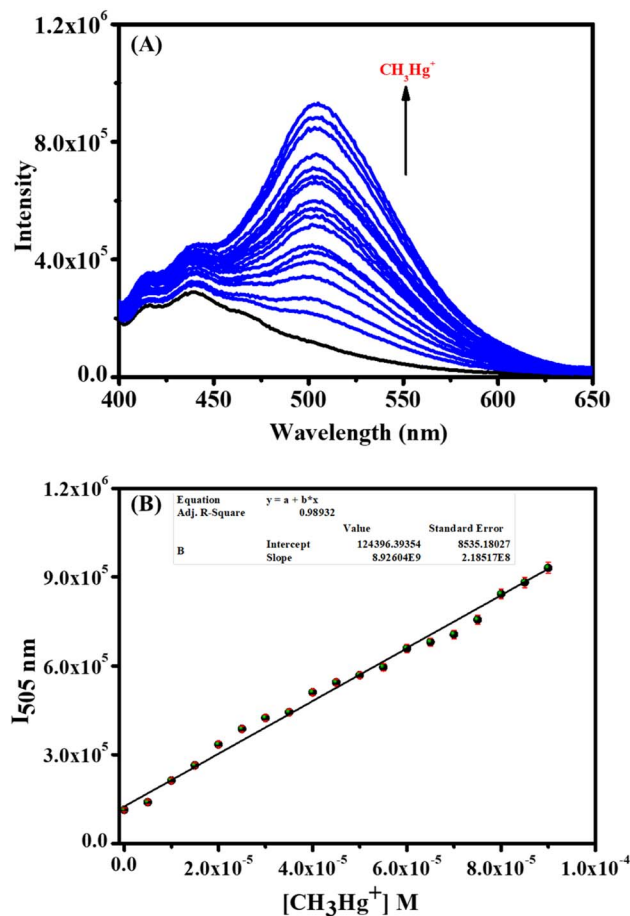


Fig. 3 Fluorescence spectra of BDT, 20  $\mu\text{M}$  (A)  $\text{CH}_3\text{Hg}^+$  (0–90  $\mu\text{M}$ ) in DMSO/PBS buffer (4 : 1, v/v, pH 7.4) solution and corresponding plot of (B)  $I_{505 \text{ nm}}$  vs concentration of  $\text{CH}_3\text{Hg}^+$  ions (0–90  $\mu\text{M}$ ) ( $\lambda_{\text{ex}} = 350 \text{ nm}$ ).

The obtained results of selectivity, response time, and LOD values suggested the superiority of the probe in comparison to various reaction-based reported fluorescent probes in recent time (Table S1, ESI<sup>†</sup>). Furthermore, all these results established the highly selective and sensitive sensing ability of the chemodosimeter BDT towards both  $\text{Hg}^{2+}$  and  $\text{CH}_3\text{Hg}^+$  in aq. media, which can be utilized to detect toxic analytes with high efficiency.

### Study of the sensing mechanism

To further validate the  $\text{Hg}^{2+}$  triggered desulfurization process of the 1,3-dithiolane moiety, we investigated the sensing mechanism by performing the  $^1\text{H}$  NMR titration experiment (Fig. 4A) of BDT in the absence and presence of  $\text{Hg}^{2+}$  ions. Upon adding excess (3 equivalent)  $\text{Hg}^{2+}$  to BDT, the protons corresponding to the 1,3-dithiolane moiety, *i.e.*, Hb and Hc, had disappeared entirely, and a new peak around 10.1 ppm appeared for  $-\text{CHO}$  groups. As a consequence of this desulfurization reaction, aromatic signals are shifted downfield. The new spectrum is identical to the  $^1\text{H}$  NMR spectrum of BDA (Fig. S1, ESI<sup>†</sup>), which firmly established the  $\text{Hg}^{2+}$  triggered desulfurization reaction of the 1,3-dithiolane moiety to form the formyl group, which activates the ESIPT process *via* keto–enol tautomerization (as



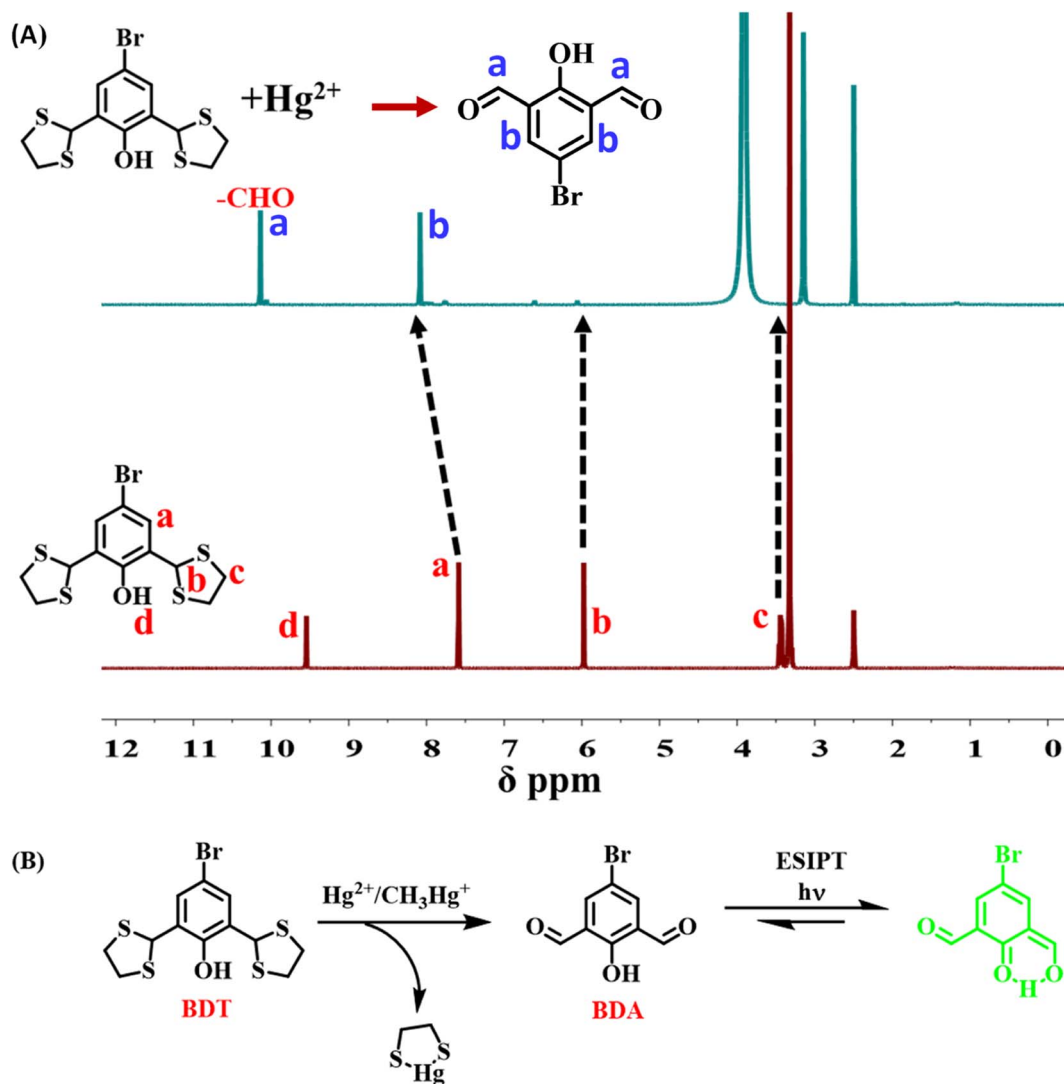


Fig. 4 (A) <sup>1</sup>H NMR spectra of BDT in the absence and presence of Hg<sup>2+</sup> in DMSO-*d*<sub>6</sub>. (B) Probable sensing mechanism of BDT for detecting Hg<sup>2+</sup> / CH<sub>3</sub>Hg<sup>+</sup>.

shown in Fig. 4B). This conversion was further supported by the similar emission spectral nature of BDA and BDT + Hg<sup>2+</sup> under identical experimental conditions (Fig. S13, ESI<sup>†</sup>). Therefore, a similar reaction process is also expected for CH<sub>3</sub>Hg<sup>+</sup> towards BDT to show the changes in emission properties, as we proved in our previous work.<sup>46</sup> This mechanism has been further supported by the ESI-MS study of BDT in the presence of Hg<sup>2+</sup> (Fig. S14, ESI<sup>†</sup>), where *m/z* = 227.195 represents the mass of BDA which confirms the desulfurization of BDT.

### Practical application ability

For practical application purposes, environmental water samples were also investigated using BDT. For this, we have collected IISER Kolkata pond water to determine Hg<sup>2+</sup> with the help of our probe BDT. However, real-life water samples contain several other competitive components, which can cause interference towards detecting Hg<sup>2+</sup> by BDT. Therefore, we have carried out the estimation of the Hg<sup>2+</sup> level with the help of the

standard addition method.<sup>47</sup> Probe BDT could quantify the added Hg<sup>2+</sup> precisely with excellent recovery (Table S2, ESI<sup>†</sup>), which entirely established the applicability of our probe towards the detection of Hg<sup>2+</sup> in real-life samples. Furthermore, to further support the relevance of our probe towards real samples, we have checked the amount of Hg<sup>2+</sup> present in commercially available powder vermilion using BDT and verified with ICP-MS (Table S2, ESI<sup>†</sup>). The obtained result suggested the excellent applicability of BDT towards the detection of Hg<sup>2+</sup> in real samples.

### Detection of Hg<sup>2+</sup> in biological samples

After confirming the precise and sensitive detection ability of BDT for Hg<sup>2+</sup> and CH<sub>3</sub>Hg<sup>+</sup>, it is essential to check the detection ability of our probe at the cellular level. Towards this, BDT has been utilized to detect Hg<sup>2+</sup> in biological systems as an incredible turn-on fluorescent probe. The initial cell viability studies of BDT revealed its low cytotoxicity effects (Fig. S14,



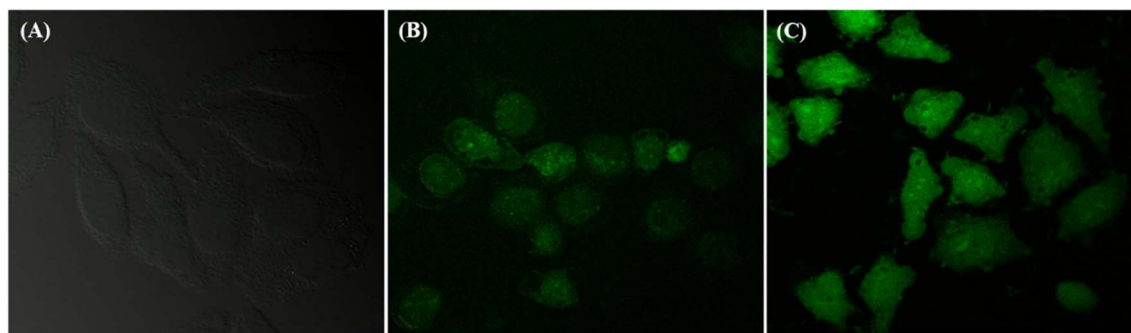


Fig. 5 Confocal laser scanning microscope images of HeLa cells pre-treated with 10  $\mu\text{M}$  BDT in the presence of (A) 0  $\mu\text{M}$ , (B) 10  $\mu\text{M}$ , and (C) 20  $\mu\text{M}$   $\text{Hg}^{2+}$  ions. Excitation wavelength: 405 nm.

ESI<sup>†</sup>). Due to having the less toxic effect of BDT on cells, we carried out a cellular imaging study by varying the  $\text{Hg}^{2+}$  ion concentration. The fluorescence intensity change of BDT in immobilized HeLa cells was investigated by changing the concentration of  $\text{Hg}^{2+}$  ions. From Fig. 5A–C, it could be easily observed that with the increasing concentration of  $\text{Hg}^{2+}$ , the fluorescence intensity of BDT tagged HeLa cells increased. These results suggested that the reaction-based fluorescence probe BDT could monitor  $\text{Hg}^{2+}$  in cells with excellent specificity and efficiency.

## Conclusion

We designed and synthesized one of the smallest, most specific, and economic reaction-based probes (BDT) to identify and quantify  $\text{Hg}^{2+}$  and  $\text{CH}_3\text{Hg}^+$  in environmental and biological samples through the 'ESIPT' activation process. BDT was demonstrated as a precise and sensitive probe for detecting inorganic and organic mercury with a theoretical detection limit of 3.8 nM and 0.8  $\mu\text{M}$ , respectively. The desulfurization reaction for the formation of dialdehyde systems was proved with the help of  $^1\text{H}$  NMR spectroscopy and fluorescence spectroscopic studies. With the capability to detect the analyte at the cellular level, we believe that BDT will provide big advantages towards detecting  $\text{Hg}^{2+}$  in biosamples. Further improvement can be made using dialdehyde systems through increased  $\pi$ -conjugation for sensing purposes, and we think that BDT will initiate this progression.

## Author contributions

T. S and N. D have equal contribution to this work. D. P and P. K performed all *in vitro* biology experiments. R. S. supervised throughout this project.

## Conflicts of interest

There is no conflict of interest.

## Acknowledgements

T. S thanks IISER-K for fellowship. N. D thanks UGC for the fellowship. P. K thanks, DBT INSPIRE for the fellowship. D. P

thanks IISER-K for the fellowship. R. S thanks IISER-K, DBT, and the Ministry of Textiles, Government of India, for funding. The authors thank IISER-K for infrastructure and facilities.

## References

- 1 M. Altrichter, Assessing potential for community-based management of peccaries through common pool resource theory in the rural area of the Argentine Chaco, *Ambio*, 2008, **37**, 108–113.
- 2 K. P. Lisha and T. Pradeep, Towards a practical solution for removing inorganic mercury from drinking water using gold nanoparticles, *Gold Bull.*, 2009, **42**, 144–152.
- 3 P. A. Ariya, M. Amyot, A. Dastoor, D. Deeds, A. Feinberg, G. Kos, A. Poulain, A. Ryjkov, K. Semeniuk, M. Subir and K. Toyota, Mercury physicochemical and biogeochemical transformation in the atmosphere and at atmospheric interfaces: A review and future directions, *Chem. Rev.*, 2015, **115**, 3760–3802.
- 4 S. L. Pan, K. Li, L. L. Li, M. Y. Li, L. Shi, Y. H. Liu and X. Q. Yu, A reaction-based ratiometric fluorescent sensor for the detection of  $\text{Hg}(\text{II})$  ions in both cells and bacteria, *Chem. Commun.*, 2018, **54**, 4955–4958.
- 5 J. García-Calvo, S. Vallejos, F. C. García, J. Rojo, J. M. García and T. Torroba, A smart material for the *in situ* detection of mercury in fish, *Chem. Commun.*, 2016, **52**, 11915–11918.
- 6 C. Song, W. Yang, N. Zhou, R. Qian, Y. Zhang, K. Lou, R. Wang and W. Wang, Fluorescent theranostic agents for  $\text{Hg}^{2+}$  detection and detoxification treatment, *Chem. Commun.*, 2015, **51**, 4443–4446.
- 7 T. W. Clarkson, L. Magos and G. J. Myers, The toxicology of mercury—current exposures and clinical manifestations, *N. Engl. J. Med.*, 2003, **349**, 1731–1737.
- 8 (a) R. Von Burg, Inorganic mercury, *J. Appl. Toxicol.*, 1995, **15**, 483–493; (b) J. Chen, J. Pan and S. Chen, A naked-eye colorimetric sensor for  $\text{Hg}^{2+}$  monitoring with cascade signal amplification based on target-induced conjunction of split DNAzyme fragments, *Chem. Commun.*, 2017, **53**, 10224–10227.
- 9 W. F. Fitzgerald, C. H. Lamborg and C. R. Hammerschmidt, Marine biogeochemical cycling of mercury, *Chem. Rev.*, 2007, **107**, 641–662.



- 10 S. Oh, J. Jeon, J. Jeong, J. Park, E. T. Oh, H. J. Park and K. H. Lee, Fluorescent detection of methyl mercury in aqueous solution and live cells using fluorescent probe and micelle systems, *Anal. Chem.*, 2020, **92**, 4917–4925.
- 11 A. Chatterjee, M. Banerjee, D. G. Khandare, R. U. Gawas, S. C. Mascarenhas, A. Ganguly, R. Gupta and H. Joshi, Aggregation-induced emission-based chemodosimeter approach for selective sensing and imaging of Hg (II) and methylmercury species, *Anal. Chem.*, 2017, **89**, 12698–12704.
- 12 V. Iyengar and J. Woittiez, Trace elements in human clinical specimens: evaluation of literature data to identify reference values, *Clin. Chem.*, 1988, **34**, 474–481.
- 13 A. T. Townsend, K. A. Miller, S. McLean and S. Aldous, The determination of copper, zinc, cadmium and lead in urine by high resolution ICP-MS, *J. Anal. At. Spectrom.*, 1998, **13**, 1213–1219.
- 14 C. B'hymer and J. A. Caruso, Arsenic and its speciation analysis using high-performance liquid chromatography and inductively coupled plasma mass spectrometry, *J. Chromatography A*, 2004, **1045**, 1–13.
- 15 K. C. Thompson and R. J. Reynolds, *Atomic Absorption. Fluorescence and Flame Emission Spectroscopy*, Charles Grifftin, London, 2nd edn, 1978, 51, pp. 175–176.
- 16 J. L. Gómez-Ariza, D. Sánchez-Rodas, I. Giráldez and E. Morales, A comparison between ICP-MS and AFS detection for arsenic speciation in environmental samples, *Talanta*, 2000, **51**, 257–268.
- 17 T. Nakazato and H. Tao, A high-efficiency photooxidation reactor for speciation of organic arsenicals by liquid chromatography–hydride generation–ICPMS, *Anal. Chem.*, 2006, **78**, 1665–1672.
- 18 D. Xu, L. Tang, M. Tian, P. He and X. Yan, A benzothiazole-based fluorescent probe for Hg<sup>2+</sup> recognition utilizing ESIPT coupled AIE characteristics, *Tetrahedron Lett.*, 2017, **58**, 3654–3657.
- 19 Y. H. Lee, H. Liu, J. Y. Lee, S. H. Kim, S. K. Kim, J. L. Sessler, Y. Kim and J. S. Kim, Dipyrrenylcalix [4] arene—a fluorescence-based chemosensor for trinitroaromatic explosives, *Chem. – Eur. J.*, 2010, **16**, 5895–5901.
- 20 M. E. Germain and M. J. Knapp, Optical explosives detection: from color changes to fluorescence turn-on, *Chem. Soc. Rev.*, 2009, **38**, 2543–2555.
- 21 A. Aliberti, P. Vaiano, A. Caporale, M. Consales, M. Ruvo and A. Cusano, Fluorescent chemosensors for Hg<sup>2+</sup> detection in aqueous environment, *Sens. Actuators, B*, 2017, **247**, 727–735.
- 22 L. Zong, Y. Xie, Q. Li and Z. Li, A new red fluorescent probe for Hg<sup>2+</sup> based on naphthalene diimide and its application in living cells, reversibility on strip papers, *Sens. Actuators, B*, 2017, **238**, 735–743.
- 23 I. Kim, N. E. Lee, Y. J. Jeong, Y. H. Chung, B. K. Cho and E. Lee, Micellar and vesicular nanoassemblies of triazole-based amphiphilic probes triggered by mercury (II) ions in a 100% aqueous medium, *Chem. Commun.*, 2014, **50**, 14006–14009.
- 24 P. Srivastava, S. S. Razi, R. Ali, R. C. Gupta, S. S. Yadav, G. Narayan and A. Misra, Selective naked-eye detection of Hg<sup>2+</sup> through an efficient turn-on photoinduced electron transfer fluorescent probe and its real applications, *Anal. Chem.*, 2014, **86**, 8693–8699.
- 25 M. H. Lee, S. W. Lee, S. H. Kim, C. Kang and J. S. Kim, Nanomolar Hg (II) detection using Nile blue chemodosimeter in biological media, *Org. Lett.*, 2009, **11**, 2101–2104.
- 26 Z. Guo, W. Zhu, M. Zhu, X. Wu and H. Tian, Near-Infrared Cell-Permeable Hg<sup>2+</sup>-Selective ratiometric fluorescent chemodosimeters and fast indicator paper for MeHg<sup>+</sup> based on tricarboyanines, *Chem. – Eur. J.*, 2010, **16**, 14424–14432.
- 27 V. Singh, P. Srivastava, S. PrakashVerma, A. Misra, P. Das and N. Singh, A new fluorescent pyrene–pyridine dithiocarbamate probe: A chemodosimeter to detect Hg<sup>2+</sup> in pure aqueous medium and in live cells, *J. Lumin.*, 2014, **154**, 502–510.
- 28 M. Y. Chae and A. W. Czarnik, Fluorometric chemodosimetry. Mercury (II) and silver (I) indication in water *via* enhanced fluorescence signaling, *J. Am. Chem. Soc.*, 1992, **114**, 9704–9705.
- 29 K. C. Song, J. S. Kim, S. M. Park, K. C. Chung, S. Ahn and S. K. Chang, Fluorogenic Hg<sup>2+</sup> selective chemodosimeter derived from 8-hydroxyquinoline, *Org. Lett.*, 2006, **8**, 3413–3416.
- 30 Y. Gao, T. Ma, Z. Ou, W. Cai, G. Yang, Y. Li, M. Xu and Q. Li, Highly sensitive and selective turn-on fluorescent chemosensors for Hg<sup>2+</sup> based on thioacetal modified pyrene, *Talanta*, 2018, **178**, 663–669.
- 31 Z. Ruan, Y. Shan, Y. Gong, C. Wang, F. Ye, Y. Qiu, Z. Liang and Z. Li, Novel AIE-active ratiometric fluorescent probes for mercury (II) based on the Hg<sup>2+</sup>-promoted deprotection of thioketal, and good mechanochromic properties, *J. Mater. Chem. C*, 2018, **6**, 773–780.
- 32 Y. Tang, D. Lee, J. Wang, G. Li, J. Yu, W. Lin and J. Yoon, Development of fluorescent probes based on protection–deprotection of the key functional groups for biological imaging, *Chem. Soc. Rev.*, 2015, **44**, 5003–5015.
- 33 P. CAS, J. Shanmugapriya, S. Singaravadeivel, G. Sivaraman and D. Chellappa, Anthracene-Based Highly Selective and Sensitive Fluorescent “Turn-on” Chemodosimeter for Hg<sup>2+</sup>, *ACS Omega*, 2018, **3**, 12341–12348.
- 34 J. Zhao, S. Ji, Y. Chen, H. Guo and P. Yang, Excited state intramolecular proton transfer (ESIPT): from principal photophysics to the development of new chromophores and applications in fluorescent molecular probes and luminescent materials, *Phys. Chem. Chem. Phys.*, 2012, **14**, 8803–8817.
- 35 (a) V. S. Padalkar and S. Seki, Excited-state intramolecular proton-transfer (ESIPT)-inspired solid state emitters, *Chem. Soc. Rev.*, 2016, **45**, 169–202; (b) J. E. Kwon and S. Y. Park, *Adv. Mater.*, 2011, **23**, 3615–3642.
- 36 J. Wu, W. Liu, J. Ge, H. Zhang and P. Wang, New sensing mechanisms for design of fluorescent chemosensors emerging in recent years, *Chem. Soc. Rev.*, 2011, **40**, 3483–3495.
- 37 S. Sahana, G. Mishra, S. Sivakumar and P. K. Bharadwaj, A 2-(2'-hydroxyphenyl) benzothiazole (HBT)–quinoline



- conjugate: a highly specific fluorescent probe for  $\text{Hg}^{2+}$  based on ESIPT and its application in bioimaging, *Dalton Trans.*, 2015, **44**, 20139–20146.
- 38 L. Deng, Y. Li, X. Yan, J. Xiao, C. Ma, J. Zheng, S. Liu and R. Yang, Ultrasensitive and highly selective detection of bioaccumulation of methyl-mercury in fish samples *via*  $\text{Ag}^0/\text{Hg}^0$  amalgamation, *Anal. Chem.*, 2015, **87**, 2452–2458.
- 39 Y. Liu, M. Chen, T. Cao, Y. Sun, C. Li, Q. Liu, T. Yang, L. Yao, W. Feng and F. Li, A cyanine-modified nanosystem for *in vivo* upconversion luminescence bioimaging of methylmercury, *J. Am. Chem. Soc.*, 2013, **135**, 9869–9876.
- 40 (a) M. Santra, B. Roy and K. H. Ahn, A “reactive” ratiometric fluorescent probe for mercury species, *Org. Lett.*, 2011, **13**, 3422–3425; (b) F. Song, S. Watanabe, P. E. Floreancig and K. Koide, Oxidation-resistant fluorogenic probe for mercury based on alkyne oxymercuration, *J. Am. Chem. Soc.*, 2008, **130**, 16460–16461; (c) L. Zhang, L. Zhang, X. Zhang, P. Liu, Y. Wang, X. Han and L. Chen, Fluorescent imaging to provide visualized evidences for mercury induced hypoxia stress, *J. Hazard. Mater.*, 2023, **444**, 130374; (d) Y. Wang, L. Zhang, X. Han, L. Zhang, X. Wang and L. Chen, Fluorescent probe for mercury ion imaging analysis: Strategies and applications, *Chem. Eng. J.*, 2021, **406**, 127166; (e) Y. Wang, M. Gao, Q. Chen, F. Yu, G. Jiang and L. Chen, Associated Detection of Superoxide Anion and Mercury(II) under Chronic Mercury Exposure in Cells and Mice Models *via* a Three-Channel Fluorescent Probe, *Anal. Chem.*, 2018, **90**(16), 9769–9778.
- 41 Y. K. Yang, S. K. Ko, I. Shin and J. Tae, Fluorescent detection of methylmercury by desulfurization reaction of rhodaminehydrazide derivatives, *Org. Biomol. Chem.*, 2009, **7**, 4590–4593.
- 42 T. Chen, T. Wei, Z. Zhang, Y. Chen, J. Qiang, F. Wang and X. Chen, Highly sensitive and selective ESIPT-based fluorescent probes for detection of  $\text{Pd}^{2+}$  with large Stokes shifts, *Dyes Pigm.*, 2017, **140**, 392–398.
- 43 Z. Huang, S. Ding, D. Yu, F. Huang and G. Feng, Aldehyde group assisted thiolysis of dinitrophenyl ether: a new promising approach for efficient hydrogen sulfide probes, *Chem. Commun.*, 2014, **50**, 9185–9187.
- 44 I. J. Chang, K. S. Hwang and S. K. Chang, Selective  $\text{Hg}^{2+}$  signaling *via* dithiane to aldehyde conversion of an ESIPT fluorophore, *Dyes Pigm.*, 2017, **137**, 69–74.
- 45 Y. Zhou, X. He, H. Chen, Y. Wang, S. Xiao, N. Zhang, D. Li and K. Zheng, An ESIPT/ICT modulation based ratiometric fluorescent probe for sensitive and selective sensing  $\text{Hg}^{2+}$ , *Sens. Actuators, B*, 2017, **247**, 626–631.
- 46 T. Samanta, N. Das, D. Patra, P. Kumar, B. Sharmistha and R. Shunmugam, Reaction-Triggered ESIPT Active Water-Soluble Polymeric Probe for Potential Detection of  $\text{Hg}^{2+}/\text{CH}_3\text{Hg}^+$  in Both Environmental and Biological Systems, *ACS Sustainable Chem. Eng.*, 2021, **9**, 5196–5203.
- 47 C. C. Huang and H. T. Chang, Selective gold-nanoparticle-based “turn-on” fluorescent sensors for detection of mercury (II) in aqueous solution, *Anal. Chem.*, 2006, **78**, 8332–8338.

